

Magnetic-field effects on the optical spectra of a carbon nanotube

Hiroshi Ajiki*

Department of Physical Science, Graduate School of Engineering Science, Osaka University, Toyonaka, Osaka 560-8531, Japan

(Received 9 January 2002; published 18 June 2002)

Magneto-optical spectra of a single-wall carbon nanotube are studied theoretically. For light polarization perpendicular to the tube axis, spectral peaks are strongly diminished by a depolarization field. In a high perpendicular magnetic field, however, clear spectral peaks remain at higher energy side from interband transition energy. For parallel polarization, the dynamical circumference current providing the depolarization field, is expected in a perpendicular magnetic field. However, the depolarization field does not appear unless an Aharonov-Bohm flux is applied.

DOI: 10.1103/PhysRevB.65.233409

PACS number(s): 78.67.Ch

Carbon nanotubes (CN's) have attracted considerable attention because of their characteristic structure of one-dimensional (1D) hollow cylinder. A CN is metallic or semiconducting, depending on the diameter and chiral arrangement of carbon atoms. In addition, magnetic flux passing through the cross section changes the band gap of a CN due to the Aharonov-Bohm (AB) effect.¹ The AB effect also affects electron transport, which has been studied for multiwall CN's.²⁻⁴ To study the remarkable band structures, the observation of optical spectra is one of the most useful experiments. In fact, structural determination of a single-wall CN was successfully done recently by resonant Raman scattering.⁵

The resonant optical transitions come from the van Hove singularities at band edges. If we apply polarized light parallel to the tube axis, clear spectral peaks corresponding to the van Hove singularities can be observed for absorption and Raman spectra. For perpendicular polarization, however, the peaks are reduced dramatically.⁶⁻¹¹ The strong reduction of the peaks originates from a depolarization field generated by current in the circumference direction.¹² Therefore the depolarization effect is crucial to discuss optical transition for CN's.

In the presence of a magnetic field perpendicular to the axis, energy levels form flat Landau levels at the Fermi level.¹ In this situation, it is not clear whether the depolarization effect for perpendicular polarization still diminishes spectral peaks or not. Furthermore, the depolarization effect is expected to occur even for parallel polarization due to the dynamical Hall effect. In the present paper we calculate magneto-optical absorption spectra of a single-wall nanotube. Although the van Hove singularities of a CN in magnetic fields have been calculated,¹³ it is insufficient to discuss optical spectra only in terms of the singularities. In fact, some peaks are shifted from resonant energy corresponding to the singularities due to the depolarization effect.

Structures of CN's are determined uniquely by chiral vectors \mathbf{L} connecting two hexagons in a 2D graphite, and L becomes the circumference length of the CN. The 2D graphite is a zero-gap semiconductor in which the valence and conduction bands consisting of π states touch at the K and K' points. The effective-mass equation around the K point is given by

$$\gamma[\sigma_x \hat{k}_x + \sigma_y \hat{k}_y] \mathbf{F}^K(\mathbf{r}) = \varepsilon \mathbf{F}^K(\mathbf{r}), \quad (1)$$

where γ is a band parameter, σ_x and σ_y are the Pauli spin matrices, $\hat{\mathbf{k}} = -i\nabla + e\mathbf{A}/c\hbar$ is the wave-vector operator in the presence of the vector potential \mathbf{A} , and \mathbf{F} is the envelope function.¹ The Fermi level lies at $\varepsilon=0$ for undoped case.

For CN's having small diameter, $\sigma^*-\pi^*$ hybridization becomes important in the electronic states.¹⁴ In the following, we consider CN's with sufficiently large diameter such that the hybridization is negligibly small. Then we have electronic states of a CN by imposing a boundary condition in the circumference direction. In the presence of an AB magnetic flux ϕ passing through the tube axis, the boundary condition is generalized as

$$\mathbf{F}^K(\mathbf{r}+\mathbf{L}) = \mathbf{F}^K(\mathbf{r}) \exp\left[2\pi i \left(\varphi - \frac{\nu}{3}\right)\right], \quad (2)$$

where $\varphi = \phi/\phi_0$ with $\phi_0 = ch/e$ being the magnetic-flux quantum. The integer ν takes 0 and ± 1 depending on the chiral vector \mathbf{L} .¹ Around the K' point the effective-mass equation and the boundary condition are obtained by replacing σ_y with $-\sigma_y$ and ν with $-\nu$.

Electronic states of a CN depend on its diameter and chirality: a CN is metallic for $\nu=0$ and semiconducting with energy gap $4\pi\gamma/3L$ for $\nu=\pm 1$. An AB flux changes the band gap ranging from 0 to $2\pi\gamma/L$ in the period of ϕ_0 .¹

Applying a magnetic field perpendicular to the tube axis, the lowest conduction and the highest valence bands approach the Fermi level, and the well-defined Landau levels are formed in a sufficiently strong magnetic field.¹ Some energy bands in a perpendicular magnetic field are shown in Fig. 1(c) and Figs. 2(b) and 2(d). In these figures the strength of the magnetic field is characterized by $L/2\pi l$, where $l = \sqrt{c\hbar/eH}$ is the cyclotron radius.

The electronic states of a CN around the K point are specified by a band index (λ, \pm) and the axial wave number k , and the corresponding energy is denoted by $\varepsilon_{\lambda K}^{(\pm)}(k)$. The “+” and “-” represent the conduction and valence bands, respectively, and we label the same indexes λ for conduction and valence bands that have mirror-symmetric relation with respect to the Fermi level, i.e., $\varepsilon_{\lambda K}^{(+)}(k) = -\varepsilon_{\lambda K}^{(-)}(k)$. We choose the x axis in the circumference direction and y in the axial direction. Then the wave function is written as

$$\mathbf{F}_{\lambda, \pm, k}^K(x, y) = \frac{1}{\sqrt{A}} \exp(iky) \bar{\mathbf{F}}_{\lambda, \pm, k}^K(x), \quad (3)$$

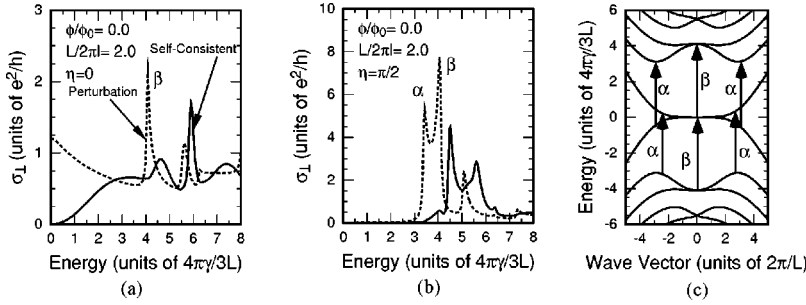


FIG. 1. Calculated absorption spectra for perpendicular polarization in perpendicular magnetic field $L/2\pi l=1.0$ with $\eta=0$ (a) and $\eta=\pi/2$ (b). Solid and dotted lines denote self-consistent results including a depolarization field and results ignoring the depolarization effect, respectively. The corresponding band structure and resonant transitions are shown in (c).

where A is the length of the CN.

Current-density operators are obtained from Eq. (1) as

$$\hat{j}_{\xi}^G(x) = \text{sgn}(G, \xi) \frac{e\gamma}{\hbar} \sigma_{\xi} \delta(\hat{x}-x), \quad (4)$$

with $G=\{K, K'\}$ and $\xi=\{x, y\}$. The $\text{sgn}(G, \xi)$ represents sign of the current-density operator, which gives $\text{sgn}(K', y) = -1$ and $\text{sgn}(G, \xi)=1$ for other combinations. The elements of the nonlocal conductivity tensor $\sigma_{\xi\xi'}(x, x')$ is written as

$$\sigma_{\xi\xi'}(x, x') = \frac{2\hbar}{iA} \sum_G \sum_{\lambda\lambda'} \sum_k \left[\frac{\langle \lambda, -, k | \hat{j}_{\xi}^G(x) | \lambda', +, k \rangle \langle \lambda', +, k | \hat{j}_{\xi'}^G(x') | \lambda, -, k \rangle}{[\varepsilon_{\lambda'G}^{(+)}(k) - \varepsilon_{\lambda G}^{(-)}(k)] [\varepsilon_{\lambda'G}^{(+)}(k) - \varepsilon_{\lambda G}^{(-)}(k) - \hbar\omega - i\Gamma]} - (x \leftrightarrow x', \omega \rightarrow -\omega) \right], \quad (5)$$

with $\langle x | \lambda, \pm, k \rangle = \bar{\mathbf{F}}_{\lambda, \pm, k}^G(x)$ and Γ being a phenomenological damping constant.

The induced current density generates the depolarization field. Since the total electric field \mathbf{E} is the sum of an external field \mathbf{D} and the depolarization field \mathbf{E}^{dep} , we obtain a self-consistent equation as follows:

$$\begin{pmatrix} E_x(l) \\ E_y(l) \end{pmatrix} = \frac{1}{\epsilon_b} \begin{pmatrix} D_x(l) \\ D_y(l) \end{pmatrix} - i \frac{|l|}{\epsilon_b} \frac{4\pi^2}{L\omega} \begin{pmatrix} j_x(l) \\ 0 \end{pmatrix}, \quad (6)$$

where the current density $j_x(l)$ defined by $j_x(x) = \sum_l j_x(l) \exp[i(2\pi l/L)x]$, is driven by the total electric field \mathbf{E} . The optical absorption is calculated as

$$P = \frac{1}{2} \frac{1}{L} \int_0^L dx \text{Re} [j_x(x) E_x^*(x) + j_y(x) E_y^*(x)]. \quad (7)$$

For simplicity, we do not consider the self-inductance effect as follows: the circumference dynamical current generates an dynamical magnetic flux that induces an electric field along the circumference direction. The self-inductance of nanotubes has been calculated in the local-field

approximation.¹⁵ In the presence of a perpendicular magnetic field, the nonlocality of the dynamical conductivity Eq. (5) becomes significant because the wave function is localized. Thus the calculation of the self-inductance should be extended in the nonlocal form.

First, we consider the optical absorption for perpendicular polarized light. The external fields are given by $D_y(l)=0$ and $D_x(l)=(D/2i)\delta_{l,1}-(D/2i)\delta_{l,-1}$ because of the sinusoidal change coming from the cylindrical geometry. From Eq. (6) we get the total field

$$E_x(l) = \frac{D}{2i} [(\Xi^{-1})_{l,1} - (\Xi^{-1})_{l,-1}], \quad (8)$$

with

$$\Xi_{ll'} = \epsilon_b \delta_{ll'} + i|l| \frac{4\pi^2}{L\omega} \sigma_{xx}(l, l') \quad (9)$$

being an effective dielectric function that includes the depolarization effect. Thus the optical absorption is given by $P_{\perp} = (D^2/2\epsilon_b^2)\sigma_{\perp}$ with

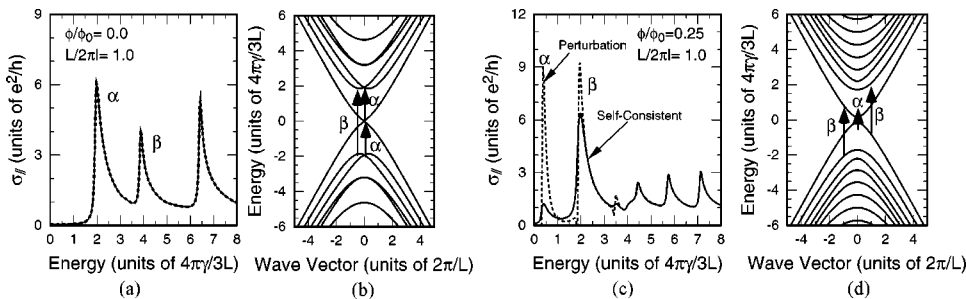


FIG. 2. Calculated absorption spectra for parallel polarization in perpendicular magnetic field $L/2\pi l=1.0$ and AB flux $\phi/\phi_0=0$ (a) and $\phi/\phi_0=0.25$. The corresponding band structures and resonant transitions are also shown in (b) and (d).

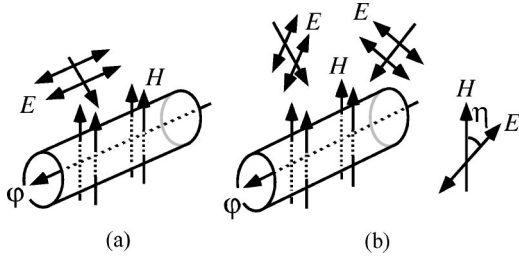


FIG. 3. Two typical arrangements for studying polarization properties of CN's in magnetic fields. (a) parallel polarization and (b) perpendicular polarization. For perpendicular polarization optical spectra depend on the angle η between E and H .

$$\sigma_{\perp} = \frac{\epsilon_b}{4} \sum_l \text{Re}\{[\sigma_{xx}(l, l) - \sigma_{xx}(-l, l)]\} \times [(\Xi^{-1})_{l,1} - (\Xi^{-1})_{l,-1}]. \quad (10)$$

Calculated absorption spectra of the metallic CN ($\nu=0$) for perpendicular polarization are shown in Fig. 1(a) for $\eta=0$ and 1(b) for $\eta=\pi/2$, where η is the relative angle between light polarization and the direction of a magnetic field [see Fig. 3(b)]. A magnetic field $L/2\pi l=2.0$ is applied in the perpendicular direction, and an AB flux ϕ is zero. Solid lines denote the results calculated from the self-consistent treatment in Eq. (10), and dotted lines correspond to the calculations ignoring the depolarization effect, i.e., effective dielectric function Ξ is replaced by $\epsilon_b \delta_{ll'}$. Figure 1(c) shows the band structure of a CN and transitions corresponding to the absorption peaks of dotted lines in Figs. 1(a) and 1(b).

In the absence of a magnetic field, optical peaks disappear for perpendicular polarization due to the depolarization effect. However, peak structures are found in a perpendicular magnetic field as is shown in Figs. 1(a) and 1(b), and the depolarization effect manifests itself as the shifts of peak energies to higher energy side. The resonating transitions occur in a strong magnetic field such that well-defined Landau levels are formed.

The absorption spectra show strong dependence on the relative angle η . In fact, the spectral peaks become more prominent for $\eta=\pi/2$ arrangement. This comes from the peculiar cylindrical shape of the CN and the localization character of the wave function in a perpendicular magnetic field. Namely, external electric field for perpendicular polarization becomes maximum at both sides of the CN because of the cylindrical shape. The wave functions of the Landau level, on the other hand, localize at the top and bottom of the CN.¹ Therefore, optical transitions occur more efficiently for $\eta=\pi/2$ than $\eta=0$.

Next we proceed to the optical absorption for parallel polarization, i.e., $D_x(l)=0$ and $D_y(l)=D\delta_{l,0}$. Although the depolarization field does not arise in the axial direction, the effective dielectric function $\Xi_{ll'}$ relates to the absorption spectra via the Hall current $j_x = \sigma_{xy} D_y$. Then the optical absorption is given by $P_{\parallel} = (D^2/2\epsilon_b^2) \sigma_{\parallel}$ with

$$\sigma_{\parallel} = \text{Re} \left[\sigma_{yy}(0,0) - i \frac{4\pi^2}{L\omega} \sum_{ll'} \sigma_{yx}(0,l) \times [(\Xi^{-1})_{ll'} |l'| \sigma_{xy}(l',0)] \right]. \quad (11)$$

Figure 2 (a) shows the calculated optical absorption of the metallic CN for parallel polarization, and the corresponding band structure is shown in Fig. 2(b). Applied magnetic fields are $L/2\pi l=1.0$ in the perpendicular direction and $\phi/\phi_0=0$ in the axial direction. The solid and dotted lines coincide with each other, and thus there exists no depolarization field in this case. However, if we apply an AB flux, large reduction of the peaks can be found in the lowest peak due to the depolarization effect, which is shown in Fig. 2(c) for $\phi/\phi_0=0.25$.

The AB flux induced depolarization effect can be demonstrated analytically. In a perpendicular magnetic field the effective-mass equation for $\bar{F}_{\lambda,+k}^K(x)$ is given by

$$\left[\sigma_x \hat{k}_x + \sigma_y \left(k_y + \frac{e}{c\hbar} A_y \right) \right] \bar{F}_{\lambda,+k}^K = \epsilon_{\lambda K}^{(+)}(k) \bar{F}_{\lambda,+k}^K. \quad (12)$$

Multiplying σ_z to the both sides of Eq. (12) from the left and inserting the identical operator $\sigma_z^2=1$ before $\bar{F}_{\lambda,+k}^K$, we find $\bar{F}_{\lambda,-k}^K = \sigma_z \bar{F}_{\lambda,+k}^K$. Similarly we apply σ_x to both sides of Eq. (12) from the left, insert $\sigma_x^2=1$ before $\bar{F}_{\lambda,+k}^K$, and apply the time reversal operator to the both sides. Then we get $\bar{F}_{\lambda,+,-k}^K = -\sigma_z \bar{F}_{\lambda,+k}^{K*}$. Combining the above results, we have also $\bar{F}_{\lambda,-,-k}^K = -\bar{F}_{\lambda,+k}^{K*}$.

Let us consider, virtual transitions $|\lambda, -, k\rangle \leftrightarrow |\lambda', +, k\rangle$ and $|\lambda', -, -k\rangle \leftrightarrow |\lambda, +, -k\rangle$ in the $\sigma_{xy}(x, x')$ of Eq. (5). From straightforward calculation using above relations on wave functions, we find the numerators of the $\sigma_{xy}(x, x')$ for two transitions have the same absolute value but opposite sign. In addition, the energy denominators of two transitions are the same. Therefore two contributions cancel out in the $\sigma_{xy}(x, x')$ even if a perpendicular magnetic field is applied. The cancellation also occurs for the contribution near the K' point in the similar way. Therefore, the depolarization field is not induced because of $\sigma_{xy}=0$.

In the presence of the AB flux, the perfect cancellation is broken and the depolarization field survives. This originates from the fact that the time reversal procedure does not lead

TABLE I. Specific strengths of magnetic fields characterized $L/2\pi l$ in the perpendicular direction (H_{\perp}) and ϕ passing through the tube axis (H_{\parallel}) for some diameters (d) of CN's. Corresponding energy gaps E_g are also listed.

d (Å)	E_g (eV) ($4\pi\gamma/3L=1$)	H_{\perp} (T) ($L/2\pi l=1$)	H_{\parallel} (T) ($\phi/\phi_0=0.25$)
10	0.82	2600	1300
20	0.41	660	330
30	0.29	290	150
60	0.14	73	38

to the relation of $\bar{F}_{\lambda,+,-k}^K = -\sigma_z \bar{F}_{\lambda,+ ,k}^{K*}$. Consequently, the AB flux gives rise to the depolarization effect for parallel polarization to the CN in a perpendicular magnetic field.

Table I shows some examples of the specific strengths of magnetic fields parallel and perpendicular to the tube axis, in which the depolarization effect on magneto-optical spectra of CN's can be found. We use the tight-binding parameter $\gamma_0 = 2.9$ eV (Ref. 5) relating to $\gamma = \sqrt{3}a\gamma_0/2$ with $a = 2.46$ Å being the lattice constant of 2D graphite. The diameter distribution of single-wall CN's ranges from ~ 10 Å to ~ 30 Å. It is difficult to confirm the present calculated results in experiments even for single-wall CN's with diameter $d = 30$ Å because an extremely strong magnetic field is needed. The depolarization effect induced by AB flux can be observed in weaker magnetic fields than listed ones; for instance, $L/2\pi l = 0.5$ ($H_{\perp} = 73$ T) and $\phi/\phi_0 = 0.2$ ($H_{\parallel} = 120$ T). Another candidate to realize the experiment is to use multiwall CN's that have large diameter for outer nanotube layers. Although it contains some CN's with different diameters in the concentric form, only the outer CN's are affected efficiently by magnetic fields. For multiwall CN's, however, we should consider depolarization fields generated by each CN. This problem will be studied in the future.

We have not consider the exciton effect of CN's. Absorption spectra including the exciton effect of single-wall CN's were calculated by Ando,¹⁶ and he pointed out that the exci-

ton bound states shift to the higher energy side because of the considerable enhancement of the band gap. The prediction was confirmed by Ichida *et al.*¹⁷ in experiment of the absorption spectra. Since many experiments support the manifestation of the depolarization effect, I believe the present results on the depolarization effect in magnetic fields are qualitatively correct even if the exciton effect is not considered.

In conclusion, we have studied magnetoabsorption spectra of a CN from the viewpoint of the depolarization effect. The depolarization effect manifests itself as shifts of absorption peaks to higher energy side for perpendicular polarized light. For parallel polarization, the depolarization effects are induced by an AB flux, and as a result, the peaks of lower side decreases considerably. The present calculation is restricted to the absorption spectra, however, the magnetic-field effects will be confirmed by resonant polarized Raman spectra also. Namely, we will find the depolarization shifts of resonating frequency of incident light for perpendicular incident light. In the case of parallel polarization, the resonant Raman intensity driven by lower resonant frequency, will be reduced by applying AB flux.

This work was supported by Scientific Research of the Ministry of Education, Science, Sports and Culture of Japan and Grant-in-Aid for COE Research (10CE2004).

*Email address: ajiki@mp.es.osaka-u.ac.jp

¹H. Ajiki and T. Ando, J. Phys. Soc. Jpn. **62**, 1255 (1993).

²A. Bachtold, C. Strunk, J.-P. Salvetat, J.-M. Bonard, L. Forró, T. Nussbaumer, and C. Schönenberger, Nature (London) **397**, 673 (1999).

³C. Schönenberger, A. Bachtold C. Strunk, J.-P. Salvetat, and L. Forró, Appl. Phys. A: Mater. Sci. Process. **69**, 283 (1999).

⁴S. Roche, F. Triozon, A. Rubio, and D. Mayou, Phys. Rev. B **64**, 121401 (2001).

⁵A. Jorio, R. Saito, J.H. Hafner, C.M. Lieber, M. Hunter, T. McClure, G. Dresselhaus, and M.S. Dresselhaus, Phys. Rev. Lett. **86**, 1118 (2001).

⁶J. Hwang, H.H. Gommans, A. Ugawa, H. Tashiro, R. Haggenmueller, K.I. Winey, J.E. Fischer, D.B. Tanner, and A.G. Rinzler, Phys. Rev. B **62**, R13 310 (2000).

⁷N. Wang, Z.K. Tang, G.D. Li, and J.S. Chen, Nature (London) **408**, 50 (2000).

⁸H.H. Gommans, J.W. Alldredge, H. Tashiro, J. Park, J. Magnusson, and A.G. Rinzler, J. Appl. Phys. **88**, 2509 (2000).

⁹A.M. Rao, A. Jorio, M.A. Pimenta, M.S.S. Dantas, R. Saito, G. Dresselhaus, and M.S. Dresselhaus, Phys. Rev. Lett. **84**, 1820 (2000).

¹⁰G.S. Duesberg, I. Loa, M. Burghard, K. Syassen, and S.P., Phys. Rev. Lett. **85**, 5436 (2000).

¹¹C. Fantini, M.A. Pimenta, M.S.S. Dantas, D. Vgarte, A.M. Rao, A. Jorio, G. Dresselhaus, and M.S. Dresselhaus, Phys. Rev. B **63**, 161405 (2001).

¹²H. Ajiki and T. Ando, Physica B **201**, 349 (1994).

¹³S. Roche, G. Dresselhaus, M.S. Dresselhaus, and R. Saito, Phys. Rev. B **62**, 16 092 (2000).

¹⁴X. Blase, L.X. Benedict, E.L. Shirley, and S.G. Louie, Phys. Rev. Lett. **72**, 1878 (1994).

¹⁵Y. Miyamoto, A. Rubio, S.G. Louie, and M.L. Cohen, Phys. Rev. B **60**, 13 885 (1999).

¹⁶T. Ando, J. Phys. Soc. Jpn. **66**, 1066 (1997).

¹⁷M. Ichida, S. Mizuno, Y. Tani, Y. Saito, and A. Nakamura, J. Phys. Soc. Jpn. **68**, 3131 (1999).